An Infiltration Method for Preparing Single Wall Nanotube/Epoxy Composites with Improved Thermal Conductivity

Fangming Du[1], Csaba Guthy[2], Takashi Kashiwagi[3], John E. Fischer[2], and Karen I. Winey[1,2 *]

[1]Department of Chemical and Biomolecular Engineering

[2]Department of Materials Science and Engineering

University of Pennsylvania, Philadelphia, PA 19104, USA

[3]Fire Research Division, National Institute of Standards and Technology, Gaithersburg, Maryland 20899, USA

Corresponding author email: winey@seas.upenn.edu

Abstract

Recent studies of SWNT/ polymer nanocomposites identify the large interfacial thermal resistance at nanotube/nanotube junctions as a primary cause for the only modest increases in thermal conductivity relative to the polymer matrix. To reduce this interfacial thermal resistance, we prepared a freestanding nanotube framework by removing the polymer matrix from a 1wt% SWNT/PMMA composite by nitrogen gasification and then infiltrated it with epoxy resin and cured. The SWNT/epoxy composite made by this infiltration method has a micron-scale bicontinuous morphology and much improved thermal conductivity (220% relative to epoxy) due to the more effective heat transfer within the nanotube-rich phase. By applying a linear mixing rule to the bicontinuous composite, we conclude that even at high loadings the nanotube framework more effectively transports phonons than well-dispersed SWNT bundles. Contrary to the widely accepted approaches, these findings suggest that better thermal and electrical conductivities can be accomplished via heterogeneous distributions of SWNT in polymer matrices.

Introduction

The structure of single wall carbon nanotubes (SWNT) produces exceptional properties and thereby SWNT is a promising filler for polymers to engineer the mechanical, electrical and thermal properties of these nanocomposites. The small diameter, large aspect ratio, and high electrical conductivity of SWNT combine to produce electrical percolation in polymer composites at extremely low loadings.[1-3] The disparity between the electrical conductivity of polymers and individual SWNT is ~20 decades and makes the electrical conductivities of SWNT/polymer composites quite sensitive to loading, alignment, and aspect ratio.[4-7] Researchers have reported electrical conductivities in SWNT/polymer composites with < 0.1 wt% SWNT that are 8 to 10 orders of magnitude higher than that of the polymer.[2,8]

In contrast, the disparity between the thermal conductivity of polymers and individual SWNT is ~10^4 W/K-m[12, 13], but the reported increases in thermal conductivity are less than a factor of two in SWNT/polymer composites.[9-11] Biercuk et al.[11] observed that their 1wt% SWNT/epoxy composite showed a 70% increase in thermal conductivity at 40K, and a 125% increase at room temperature. These reported enhancements are nearly negligible considering the large thermal conductivity of individual SWNT, ~10^3 W/K-m.[12,13] Researchers attribute these unexpectedly small increases in thermal conductivity to a large interfacial thermal resistance at the nanotube/polymer interface.[14,15] Previous attempts to improve thermal conductivity have focused on uniformly dispersing SWNT in a polymer matrix, which works well for electrical conductivity. In this paper, we present a new fabrication method that improves thermal conductivity by creating a heterogeneous distribution of SWNT, specifically an interconnected SWNT-rich phase within an epoxy matrix.

Experimental Methods

Our poly(methyl methacrylate) (PMMA) was purchased from Polyscience Inc. with M_w of 100,000g/mol, and the thermoset epoxy was EPON Resin 862 (bisphenol F) from Resolution with an unmodified cycloaliphatic amine (Amicure PACM) from Air Products as curing agent. The SWNT were synthesized by the HiPco process[16] and were provided by Carbon Nanotechnologies Incorporated. Our coagulation method[6] was used to produce the SWNT/PMMA nanocomposites with various loadings, providing a uniform dispersion of small SWNT bundles in the matrix. The 1wt% SWNT/PMMA nanocomposite was then hot pressed into a 75 mm diameter and 4 mm thick disk for nitrogen gasification, which was done in a radiant gasification apparatus.[17, 18] A well-mixed epoxy resin and curing agent (3:1 by weight) was infiltrated into the residue of the 1wt% nanocomposite after nitrogen gasification at room temperature under vacuum. A two-stage curing process was used to produce the SWNT/epoxy composite: 80ºC for 2 h and 150ºC for 2 h.

Optical microscopy (Olympus, BH-2) was used to characterize the morphologies of the fracture surface of the SWNT/epoxy composites. Scanning electron microscopy (SEM) (JEOL 6300FV, at 5kV) was performed on the fracture surface of the SWNT/epoxy composite and on the SWNT residue after nitrogen gasification of the SWNT/PMMA composite. Electrical conductivities greater than 10^{-2} S/cm were measured by a four-probe method at room temperature, while smaller conductivities were measured by a two-probe method at room temperature using a high impedance electrometer (Keithley Model 616). Thermal conductivity experiments were conducted at room temperature using a comparative method.[19] Small samples (approximately 2 mm × 2 mm × 2 mm) were mounted in series with constantan rods of known temperature-dependent thermal conductance. Heat was transferred from the heating source to the

first constantan rod to the sample to the second constantan rod to the cold stage. Differential thermocouples were attached directly to the sample and the constantan rods to measure the two sample-constantan temperature drops from which we calculate the thermal conductivity of the sample approximately corrected for radiation losses by averaging the two[19].

Results and Discussion

As expected, our isotropic SWNT/PMMA composites made by the coagulation method[6] show a percolation behavior in electrical conductivity with increasing SWNT loading, Figure 1a. The conductivities of these nanocomposites increase sharply over the range from 0.3 to 0.5wt% SWNT loading, indicating a percolation threshold of ~0.3wt%. The nanocomposite with 2wt% SWNT has an electrical conductivity of ~10^{-3} S/cm, which is ~10^{12} times higher than that of pure PMMA, 10^{-15} S/cm. In contrast, the thermal conductivity of this electrically conductive nanocomposite is 0.18 W/Km and comparable to that of pure PMMA, Figure 1b. There is no significant increase in thermal conductivity for the nanocomposites with loadings up to 5wt%, and increasing to 7wt% SWNT only produces a factor of two increase.

SWNT/polymer composites above the critical percolation concentration have continuous nanotube pathways that allow electrons to travel, but these nanotube pathways are insufficient for thermal conductivity, because electricity and heat transport occur by distinct mechanisms. An electron hopping mechanism has been adopted to describe the electrical conductivity of the nanotube/polymer nanocomposites. This mechanism requires close proximity (~5 nm) of the nanotubes or nanotube bundles in the nanocomposites and direct nanotube contact is unnecessary.[3] The electrical resistance associated with electron hopping between SWNT contributes to the ~6 orders of magnitude difference in electrical conductivity between a 2wt%

composite (~10^{-3} S/cm) and a SWNT buckypaper (~10^{3} S/cm).[20] (Nanotube buckypaper is produced by filtering a nanotube suspension to form a freestanding, all-nanotube film.) This electron hopping SWNT-SWNT electrical resistance is negligible compared to the SWNT-polymer electrical resistance, such that electrons reside primarily on SWNT and the hopping mechanism dominates electrical conduction through the composite.

Heat transport along isolated nanotubes occurs by phonons with a wide range of frequencies; in nanotube/polymer nanocomposites this requires phonon transfer from tube to tube *via* the polymer.[19] Due to the difference in stiffness, the nanotubes and the polymer matrix are coupled by only a small number of low-frequency vibrational modes in the absence of covalent bonds at the interface. Thus, thermal energy contained in high-frequency phonon modes within the nanotubes must first be transferred to low-frequency phonons through phonon-phonon couplings before being exchanged with the surrounding medium. This is the origin of the high interfacial thermal resistance in nanotube/polymer composites. Huxtable et al.[14] used picosecond transient absorption to measure the interfacial thermal conductance of carbon nanotubes suspended in surfactant micelles in water (~12 $MWm^{-2}K^{-1}$), a system comparable to polymer-based nanocomposites. Similar results were also obtained from molecular dynamics simulations[21] of heat flow between a carbon nanotube and liquid octane. These results indicate that heat transport in nanotube/polymer nanocomposites will be limited by (1) the exceptionally small interface thermal conductance at nanotube/nanotube junctions that contain even a small amount of intervening polymer and (2) the modest thermal conductance of intimate nanotube/nanotube junctions. This is in marked contrast to electrical conduction where the electron hopping mechanism can readily transfer electrons even when the nanotubes are separated by a small amount of polymer.

The distinction between nanotube/polymer/nanotube and intimate nanotube/nanotube junctions is somewhat arbitrary, but is meant to illustrate that phonons can be transferred from one nanotube to the next with or without the intermediate step of phonon transfer to the polymer. This further implies multiple values for the interfacial resistance in these composites. One consequence of this distinction is that while nanotube/polymer/nanotube junctions might be eliminated, for example by thermally degrading the polymer, nanotube/nanotube junctions will persist. Thus, predicting the thermal conductivity of SWNT/polymer nanocomposites by using the polymer and isolated SWNT thermal conductivities as the limits is overly optimistic because it ignores the nanotube/nanotube junctions. If we consider SWNT buckypaper as a SWNT/air composite without nanotube/polymer/nanotube junctions, we find that the nanotube/nanotube thermal conductance is considerably smaller than isolated SWNT. Hone et al.[13] found the thermal conductivity of SWNT buckypaper at room temperature to be ~10 to ~30 W/m-K; the value depends on SWNT alignment. The drop from ~10^3 W/m-K for individual SWNT to ~10^1 W/m-K for SWNT buckypaper is primarily attributed to the thermal resistance at various types of nanotube/nanotube junctions.

Rather than increase the thermal conductance at nanotube/nanotube junctions, our efforts have focused on reducing the number of nanotube/polymer/nanotube junctions. In principle this could be accomplished by increasing the nanotube loading, but the viscosity of thermoplastics with high concentrations of discrete SWNT and small SWNT bundles increases dramatically and inhibits processing.[3] Alternatively, we have developed a fabrication method that creates an open nanotube framework in which all the junctions are nanotube/nanotube in nature. Then a polymer matrix is synthesized in situ by infiltrating the nanotube framework with a chemical precursor

and heating to drive the chemical reaction. The result is a composite with small nanotube loading and higher thermally conductivity.

Figure 2 schematically shows the infiltration method using a nanotube framework. The process begins with the electrically conductive 1wt% SWNT/PMMA nanocomposite made by the coagulation method. During nitrogen gasification[18] the PMMA matrix reverts to methyl methacrylate monomers that leave the nanocomposite in the gas phase. The residue of this thermal degradation process is a robust and freestanding nanotube framework with nanotube/nanotube junctions, Figure 3. This SWNT residue was infiltrated with premixed epoxy resin and curing agent using a room temperature vacuum and then cured. We estimate the SWNT loading in the resulting SWNT/epoxy to be ~2.3wt%, because the nanotube residue (~3.5 mm) is thinner than the 1wt% SWNT/PMMA sample before gasification (8 mm). (Note that TGA could not be used to establish the SWNT/epoxy composition due to overlapping degradation temperature regimes.) The 2.3wt% SWNT/epoxy composite has an average thermal conductivity ~0.61 W/Km, a ~220% increase relative to both pure epoxy and PMMA. For comparison, a 2wt% SWNT/PMMA composite prepared from discrete SWNT bundles via the coagulation method exhibits only ~20% enhancement in thermal conductivity. The electrical conductivities of these 2.3wt% SWNT/epoxy and 2 wt% SWNT/PMMA composites are 1.4 and ~10^{-3} S/cm.

There are significant morphological differences between the composites prepared by coagulation and infiltration; these differences affect both the electrical and thermal conductivities at a fixed SWNT loading. As previously reported, rapid coagulation prevents the agglomeration of SWNT, so the dispersion of SWNT in the processing solvent is representative of the spatial distribution of SWNT in the polymer matrix. In the case of HiPco SWNT in the solvent, the SWNT are in small bundles of ~10 nanotubes. Thus, at low SWNT loadings phonons must transfer from the nanotubes to the polymer matrix and back to the nanotubes and thereby

encounter the high interfacial resistances. Vacuum infiltration of epoxy resin into the SWNT framework produces a bicontinuous structure with nanotube-rich pathways surrounded by the epoxy matrix, Figure 4. Optical microscopy shows that the nanotube-rich pathways connect opposite sides of the sample, and SEM shows that within these pathways, the nanotubes have many close contacts with one another. Phonons will travel preferentially in the high SWNT density regions where there are fewer nanotube/polymer/nanotube junctions, resulting in a higher composite thermal conductivity.

Predictions of thermal conductivity of nanotube/polymer nanocomposites are generally based on discrete nanotubes and nanotube bundles. Guthy et al.[23] used the Nielsen model[24] to fit SWNT composite data; this revealed a strong dependence of thermal conductivity on filler aspect ratio. An analytic model developed by Nan et al.[15] can be applied below the percolation threshold and incorporates an interfacial thermal resistance. In contrast, we apply a linear mixing rule to our bicontinuous SWNT/epoxy composite where heat transfer occurs through two isotropic and micron-sized media, the pure epoxy and the nanotube-rich pathway (*nrp*):

$$\kappa_{comp} = x_{nrp}\kappa_{nrp} + (1 - x_{nrp})\kappa_{epoxy} \qquad (1)$$

where κ_{comp}, κ_{nrp}, and κ_{epoxy} are thermal conductivities of the composite, the nanotube-rich pathway, and the epoxy respectively, and x_{nrp} is the volume fraction of the nanotube-rich pathway. The latter is 0.12 ± 0.03, as measured using the optical micrographs of the fracture surface and a line fraction method. (The line fraction method capitalizes on the equivalence of line fraction and volume fraction in an isotropic specimen by equating the fraction of a line on a micrograph that overlaps the nanotube-rich pathway equals the volume fraction.) Having measured κ_{comp} and κ_{epoxy} with the comparator method, we use Eq.1 to find κ_{nrp} = 3.8 W/m-K.

By mass balance, we estimate the SWNT mass fraction in the nanotube-rich pathways to be 2.3wt% / 12% = 20wt%. (The SWNT volume fraction is assumed to be equal to the weight fraction because the densities of both epoxy and SWNT are similar, 1.2 g/cm^3 for epoxy and ~1.3 g/cm^3 for SWNT.)

Figure 5 compares the thermal conductivities for a variety of composites, including the nanotube-rich pathway, by plotting the relative thermal conductivity (κ_{comp} / κ_m) as a function of nanotube loading, Figure 5. At low loadings, the bicontinuous SWNT/epoxy composite has higher thermal conductivity than the SWNT/PMMA composites with well-dispersed SWNT. In a separate study we prepared SWNT/polyethylene composites using an adaptation of the coagulation method with up to 30wt% SWNT.[25] The improvement in thermal conductivity in the nanotube-rich pathway with 20wt% SWNT prepared by nitrogen gasification is greater than in the 30wt% SWNT/PE composite containing discrete SWNT. This illustrates the importance of reducing nanotube/polymer/nanotube contacts to increase the thermal conductivity in composites even at high SWNT loadings.

The bicontinuous morphology produced by our infiltration method improves both electrical and thermal conductivities by ensuring *poor* SWNT dispersion. This contradicts the widely accepted approach that better conductivities in nanocomposites will be achieved through better SWNT dispersion. Other evidence that inhomogeneous nanocomposites exhibit better conductivities has been reported. Bryning et al.[8] found that SWNT aggregation helps electrical conductivity of their SWNT/epoxy composite and Martin et al.[22] showed that relatively poor multi wall carbon nanotube dispersion leads to a lower electrical percolation threshold. This insight might inspire new approaches to fabricating composites that have bicontinuous morphologies with a nanotube-rich phase. While nitrogen gasification was used in this study,

more practical approaches could be developed to prepare freestanding nanotube frameworks for infiltration with epoxy, and other matrices compatible with bulk polymerization. This strategy of forming a nanotube framework with nanotube/nanotube junctions with low thermal resistance and then infiltrating with a polymer precursor will provide improved thermal conductivity at significantly lower (< 5wt%) nanotube loading.

Conclusions

SWNT/PMMA composites made by coagulation exhibit percolation behavior in electrical conductivity but no significant improvement in thermal conductivity, which highlights the contrasting mechanisms of electrical and thermal transport. Large interfacial thermal resistances at nanotube/polymer/nanotube junctions contribute to the low thermal conductivity of SWNT/polymer composites. To reduce this interfacial thermal resistance, we prepared a freestanding nanotube framework by removing the polymer matrix from a 1wt% SWNT/PMMA composite using nitrogen gasification, and then infiltrated it with epoxy resin and cured. The resulting SWNT/epoxy composite has a micron-sized bicontinuous morphology and exhibits much improved thermal conductivity due to the more effective heat transfer within the nanotube-rich phase. By applying a linear mixing rule to the bicontinuous composite and normalizing for the higher SWNT loading, we conclude that the nanotube rich phase more effectively transports phonons than well-dispersed SWNT bundles.

The fabrication method presented here could be extended. For example, freestanding nanotube frameworks might be prepared by alternative routes to reduce the number of steps, perhaps by developing a sol-gel process. Furthermore, while this paper demonstrates the concept

with epoxy, this infiltration method is broadly applicable to various thermoplastics and thermosets, as long as the volume change upon polymerization or curing is small.

Acknowledgement

We acknowledge useful discussion and help from R. Haggenmueller and T. Acchione of the Department of Materials Science and Engineering at the University of Pennsylvania. Funding for this research was provided by the National Science Foundation (DMR-MRSEC 05-20020) and the Office of Naval Research (N00014-03-1-0890 and DURINT N00014-00-1-0720).

Reference

1. Benoit, J. M.; Corraze, B.; Chauvet, O. *Physical Review B* **2002,** 65, 24140501-24140504.

2. Barrau, S.; Demont, P.; Perez, E. *Macromolecules* **2003,** 36, 9678-9680.

3. Du, F.; Scogna, R. C.; Zhou, W.; Brand, S.; Fischer, J. E.; Winey, K. I. *Macromolecules* **2004,** 37, (24), 9048-9055.

4. Benoit, J. M.; Corraze, B.; Lefrant, S.; Blau, W.; Bernier, P.; Chauvet, O. *Synthetic Metals* **2001,** 121, 1215-1216.

5. Bai, J. B.; Allaoui, A. *Composites Part A: Applied Science and Manufacturing* **2003,** 34, 689-694.

6. Du, F.; Fischer, J. E.; Winey, K. I. *Journal of Polymer Science: Part B: Polymer physics* **2003,** 41, (24), 3333-3338.

7. Du, F.; Fischer, J. E.; Winey, K. I. *Physical Review B* **2005,** 72, 12140401-04.

8. Bryning, M. B.; Islam, M. F.; Kikkawa, J. M.; Yodh, A. G. *Advanced Materials* **2005,** 17, (9), 1186-1191.

9. Kashiwagi, T.; Grulke, E.; Hilding, J.; Groth, K.; Harris, R.; Shields, J.; Kathryn, B.; Kharchenko, S.; Douglas, J. *Polymer* **2004,** 45, (12), 4227-4239.

10. Choi, E. S.; Brooks, J. S.; Eaton, D. L.; Al-Haik, M. S.; Hussaini, M. Y.; Garmestani, H.; Li, D.; Dahmen, K. *Journal of Applied Physics* **2003,** 94, (9), 6034-6039.

11. Biercuk, M. J.; Llaguno, M. C.; Radosavljevic, M.; Hyun, J. K.; Johnson, A. T.; Fischer, J. E. *Appl. Phys. Lett.* **2002,** 80, (15), 2767-2739.

12. Zhong, H.; Lukes, J. R. *Proceedings of IMECE* **2004**.

13. Hone, J.; Batlogg, B.; Benes, Z.; Llaguno, M. C.; Nemes, N. M.; Johnson, A. T.; Fischer, J. E. *Materials Research Society Symposium Proceedings* **2001,** 633, A17.1.1-A17.1.12.

14. Huxtable, S. T.; Cahill, D. G.; Shenogin, S.; Xue, L.; Ozisik, R.; Barone, P.; Usrey, M.; Strano, M. S.; Siddons, G.; Shim, M.; Keblinski, P. *Nature Materials* **2003,** 2, 731-734.

15. Nan, C.; Liu, G.; Lin, Y.; Li, M. *Applied Physics Letters* **2004,** 85, (16), 3549-3551.

16. Bronilowski, M. J.; Willis, P. A.; Colbert, D. T.; Smith, K. A.; Smalley, R. E. *Journal of Vacuum Science and Technology A* **2001,** 19, (4), 1800-1805.

17. Kashiwagi, T.; Du, F.; Douglas, J. F.; Winey, K. I.; Harris, R. H.; Shields, J. R. *Nature Materials* **2005,** 4, (12), 928-933.

18. Kashiwagi, T.; Du, F.; Winey, K. I.; Groth, K. M.; Shields, J. R.; Bellayer, S. P.; Kim, H.; Douglas, J. F. *Polymer* **2005,** 46, (2), 471-481.

19. Hone, J.; Whitney, M.; Piskoti, C.; Zettl, A. *Physical Review B* **1999,** 59, (4), 2514-2516.

20. Fischer, J. E.; Zhou, W.; Vavro, J.; Llaguno, M. C.; Guthy, C.; Haggenmueller, R.; Casavant, M. J.; Walters, D. E.; Smalley, R. E. *Journal of Applied Physics* **2003,** 93, (4), 2157-2163.

21. Shenogin, S.; Xue, L.; Ozisik, R.; Keblinski, P. *Journal of Applied Physics* **2004,** 95, (12), 8136-8144.

22. Martin, C. A.; Sandler, J. K. W.; Shaffer, M. S. P.; Schwarz, M. K.; Bauhofer, W.; Schulte, K.; Windle, A. H. *Composites Science and Technology* **2004,** 64, (13), 2309-2316.

23. Guthy, C.; Du, F.; Brand, S.; Fischer, J. E.; Winey, K. I. *Materials Research Society Symposium Proceedings* **2005,** 858E, HH.3.31.1-6.

24. Nielsen, L. E. *Journal of Applied Polymer Science* **1973,** 17, (13), 3819-3820.

25. Haggenmueller, R.; Lukes, J.R.; Fischer, J.E.; Winey, K.I., *Macromolecules* in preparation.

Figure Captions:

Figure 1: (a) Electrical conductivity and (b) thermal conductivity as function of SWNT loading for the PMMA nanocomposites made by the coagulation method. Thermal conductivity is accurate to +/- 15%.

Figure 2: Schematic of the infiltration method.

Figure 3: (a) Photograph and (b) SEM image of the 1% SWNT/PMMA residue after nitrogen gasification.

Figure 4: (a) Optical and (b) SEM image of the SWNT/epoxy composite fabricated by the infiltration method.

Figure 5: The ratio of thermal conductivity of SWNT/polymer composite to its polymer matrix as a function of SWNT loading. (■) SWNT/PMMA composites made by the coagulation method using discrete SWNT bundles; (▲) SWNT/epoxy composite made by the infiltration method using a freestanding SWNT network produced by nitrogen gasification; (♦) the nanotube-rich region of the SWNT/epoxy composite as calculated from the linear mixing rule; and (□) SWNT/PE composite using discrete SWNT bundles (data from R. Haggenmueller et al.[25]). Dotted line is $\kappa/\kappa_m=1$. Thermal conductivity is accurate to +/- 15%.

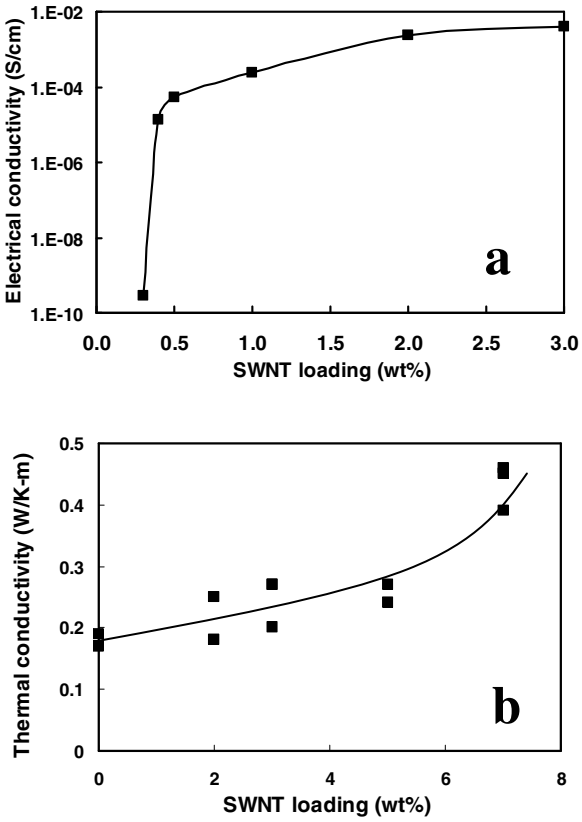
Electrical conductivity (S/cm)
1.E-02
1.E-04
1.E-06
1.E-08
1.E-10
0.0
0.5
1.0
1.5
2.0
2.5
3.0
SWNT loading (wt%)
a
Thermal conductivity (W/K-m)
0.5
0.4
0.3
0.2
0.1
0
0
2
4
6
8
SWNT loading (wt%)
b

Figure 1

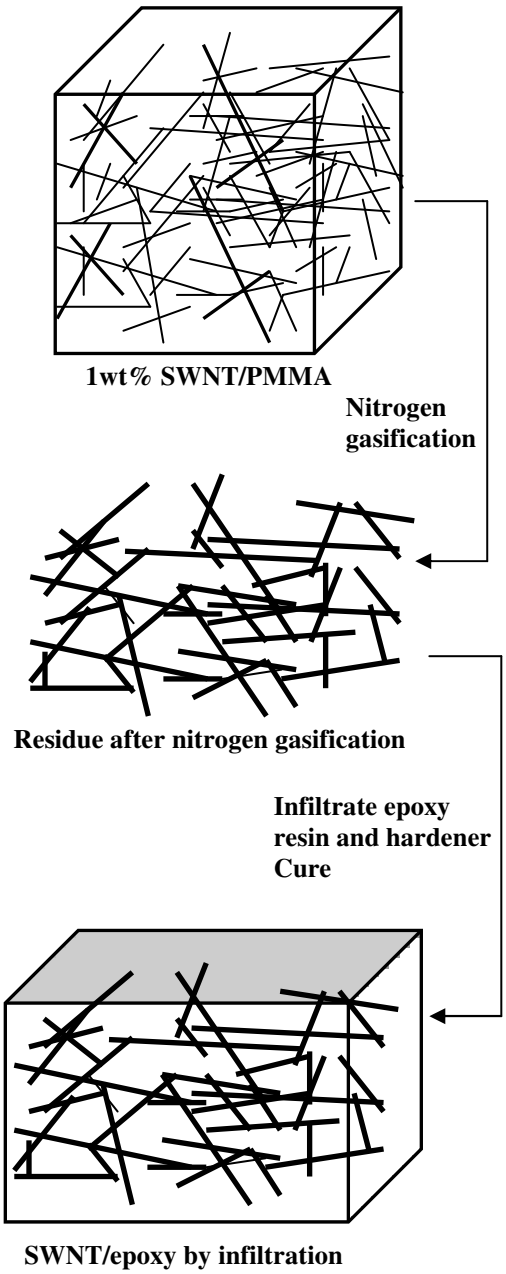
1wt% SWNT/PMMA
Nitrogen
gasification
Residue after nitrogen gasification
Infiltrate epoxy
resin and hardener
Cure
SWNT/epoxy by infiltration

Figure 2

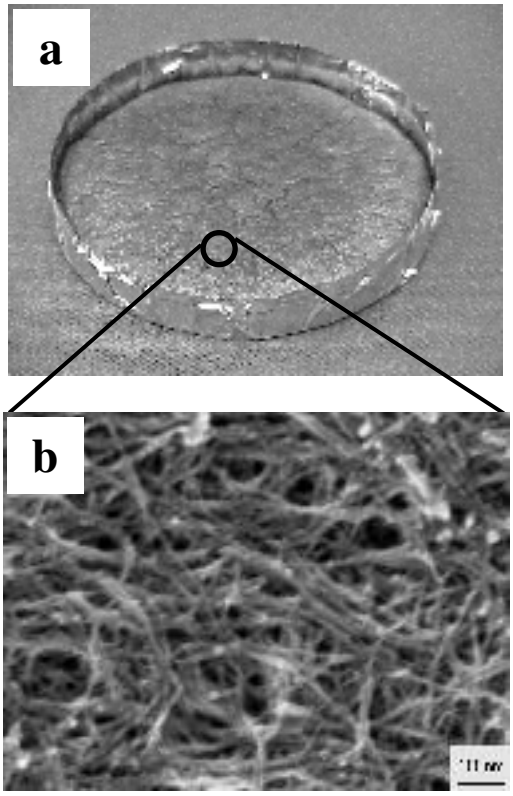

Figure 3

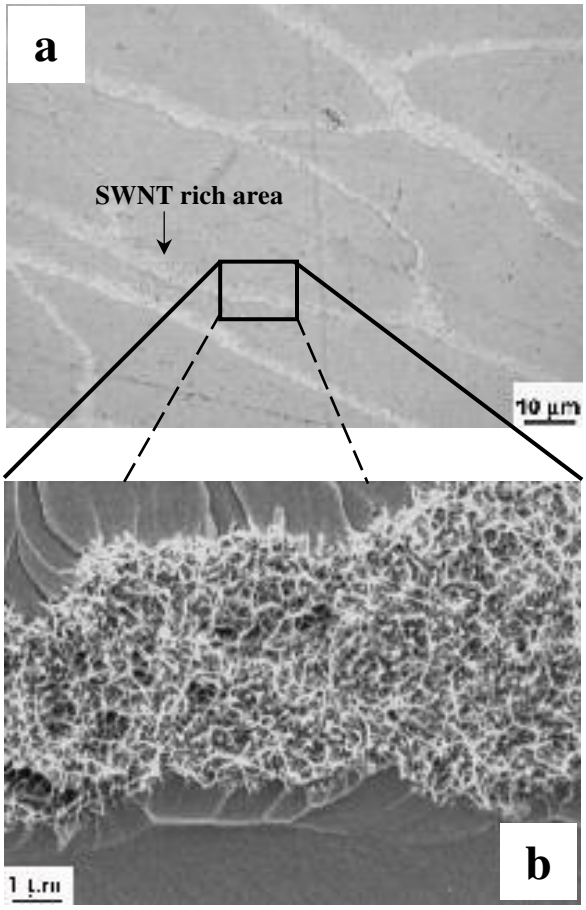

Figure 4

\

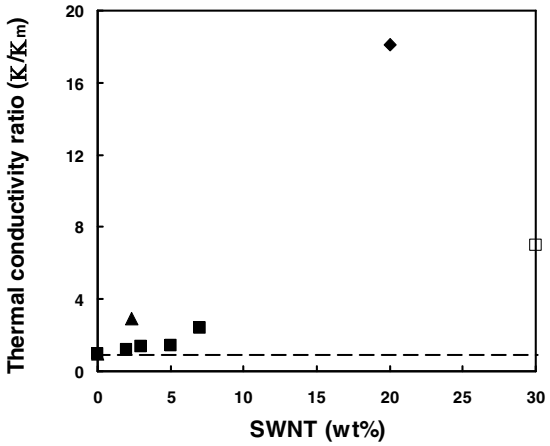
Thermal conductivity ratio (K/Km)
SWNT (wt%)
0
4
8
12
16
20
0
5
10
15
20
25
30

Figure 5